BedloadBedrock Contrasts Form Enigmatic LowRelief Surfaces of the Pyrenees

Geophysical Research Letters

RESEARCH LETTER
10.1029/2022GL101995

Key Points:

- Bedload-bedrock contrasts allow for a strong lithological control without a clear geomorphic fingerprint
- Steady state tectonic forcing with variable lithology can produce low-relief Pyrenean surfaces

Correspondence to:

M. Fox,
m.fox@ucl.ac.uk

Citation:

Fox, M., Hoseason, T., Bernard, T., Sinclair, H., & Smith, A. G. G. (2023). Bedload-bedrock contrasts form enigmatic low-relief surfaces of the Pyrenees. *Geophysical Research Letters*, *50*, e2022GL101995. https://doi.org/10.1029/2022GL101995

Received 3 NOV 2022
Accepted 1 JAN 2023

Bedload-Bedrock Contrasts Form Enigmatic Low-Relief Surfaces of the Pyrenees

M. Fox[1], T. Hoseason[1], T. Bernard[2], H. Sinclair[2], and A. G. G. Smith[1,3]

[1]A Department of Earth Sciences, University College London, London, UK, [2]School of GeoSciences, The University of Edinburgh, Edinburgh, UK, [3]Department of Earth & Planetary Science Birkbeck, University of London, London, UK

Abstract Low-relief, high-elevation surfaces in mountain belts highlight the dynamic nature of landscapes and have provided evidence for changes in tectonics and/or climate. Yet quantifying when changes occurred from topographic data is challenging and relationships between erosion rate, lithology and precipitation are complex. In the Pyrenees, low-relief, high elevation surfaces are found across both plutonic massifs and the surrounding softer rocks and channel steepness values are relatively uniform between these lithologies. This suggests a weak relationship between erosion rate and lithology despite a clear relationship between the drainage network configuration and the location of the plutonic rocks. We explore this conflicting evidence for strength of the relationship between lithology and erosion rate using a landscape evolution model which accounts for the contrast between bedrock and bedload erodibility. This contrast produces dispersed channel steepness values and predicts the in situ development of low-relief surfaces, under steady forcing conditions.

Plain Language Summary Unusual landscapes provide an indication that processes shaping Earth's surface have changed. In this way, features of the topography can be used to understand the past. However, the processes shaping the surface are complicated. In the Pyrenees, there are unusual, low-slope topographic features at high elevations, where we would expect to find steep slopes. One explanation of these low-slope features is that they have recently been uplifted from low elevations to high elevations. This would require large changes in tectonics. Here we explore whether changes in exposed rock type might produce these low-slope regions. Because there is no clear indication that exposed rock type might lead to changes in the patterns of drainage networks, we suggest that the exposure of different rock types change the bedload of rivers. This evolving bedload produces complex incision patterns, disrupting the river network and producing low-slope, high elevation surfaces.

1. Introduction

Enigmatic low-relief, high elevation surfaces (LRHES) are found in many mountainous landscapes and have been the subject of debate since early work by Davis (1899). These surfaces indicate geomorphic processes have changed at some time in the past driven by tectonics, climate and drainage network reorganization. Constraining the timing of these changes by extracting erosion rates from topographic data is challenging, in part because the relationships amongst lithology, precipitation and sediment transport are uncertain. These LRHES features are found across the Pyrenees (Figure 1), and form relatively smooth interpolated surfaces with elevations up to 2,800 m asl in the Axial Zone (Babault et al., 2005; de Sitter, 1952; England & Molnar, 1990). On the one hand, these surfaces are hypothesized to have formed during a prolonged period of erosion resulting in a low-relief, low-elevation landscape that was uplifted and dissected in the Pliocene (e.g., de Sitter, 1952; Gunnell et al., 2008); the evidence for this is primarily from the eastern Pyrenees. On the other, these surfaces are argued to have formed in response to filling of sedimentary basins, locally elevating the baselevel of rivers draining the Pyrenees and thereby forming a low-relief, high-elevation landscape (Babault et al., 2005; Bernard et al., 2019; Bosch et al., 2016). These hypotheses represent simplifications of complex concepts but highlight that the geodynamic and geomorphological implications of these two end-member hypotheses is stark.

The LRHES across the Pyrenees have been described as remnants of a single composite peneplanation surface that has been dissected (Babault et al., 2005; Bosch et al., 2016; Calvet, 1996; de Sitter, 1952). This surface cuts through different lithologies and tectonic structures and is occasionally overlain by Oligocene and Upper Miocene continental deposits in the southern and northern sides respectively, providing constraints on the age for its development (Cabrera et al., 1988; Roca, 1996; Ortuño et al., 2008, 2013). The surfaces on the southern

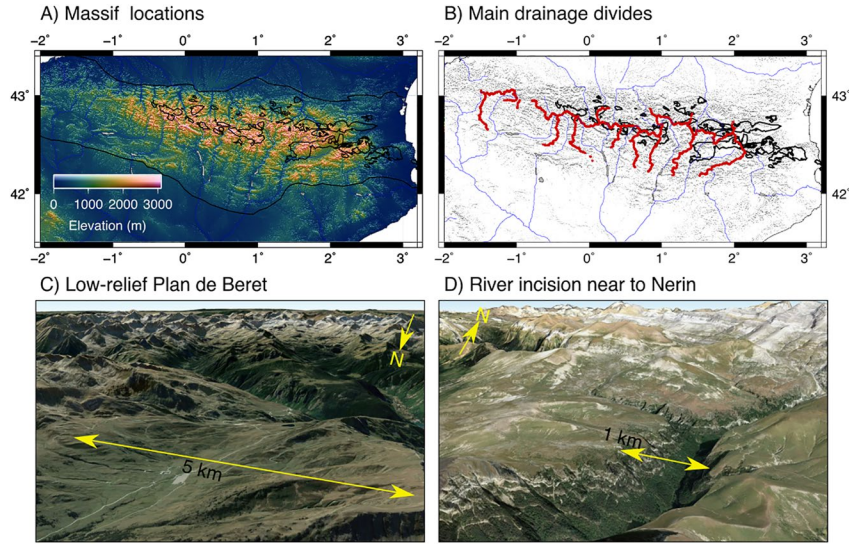

Figure 1. The topography of the Pyrenees. (a) The massifs of the Pyrenees are located within the center of the orogen, black outlines. Digital elevation data from Hydrosheds (Lehner et al., 2008). This zone is referred to as the Axial Zone. High elevations are found within the Axial Zone however, there is no clear correlation with lithology. (b) The tortuous path of the main drainage divides appear to coincide with the locations of the plutonic rocks as quantified by Bernard et al. (2019). (c) An example of a debated low-relief surface, the Plan de Beret. This surface is at an elevation of ∼1,850 m and steep topography is identified below and above the surface. Image from Google Earth. (d) Differential erosion is observed across the Pyrenees as highlighted by this active incision into a relatively low-relief surface near to Nerin. Image from Google Earth.

side of the range are well correlated up to approximately 1,800 m, with small remnants continuing up to 2,900 m (Babault et al., 2005; Bosch et al., 2016). On the northern side, a similar concentration of surfaces are correlated up to around 800 m (Bernard et al., 2019). Interpolating a continuous surface through LRHES suggests that they potentially originate from a gently undulating landscape (Bosch et al., 2016).

Geomorphic and geodynamic arguments have been put forward to refute the two leading scenarios. For the first scenario, in which peneplanation occurred around 800 m and drained directly to sea-level, followed by a subsequent increase in rock uplift, there is limited evidence for enhanced crustal thickening or removal of mantle lithosphere below the central Pyrenees (Bosch et al., 2016). For the second scenario, in which the surface formed at high elevation in response to continued erosion and sediment aggradation along the Pyrenean piedmonts, it is unclear whether such a large amount of aggraded sediment could be efficiently evacuated without record (Gunnell & Calvet, 2006). Recent work investigating sediment transport from a flexural isostatically compensated orogen to a coupled foreland basin suggests that some sediment drape and aggradation is expected as seen on the northern Pyrenees, but not to the highest elevations of the observed surfaces (Bernard et al., 2019). In addition, the sediment load associated with this aggradation would lead to significant flexural deflection of lithospheric plates, yet the overall load of the central Pyrenean topography has remained relatively constant since the Oligocene (Curry et al., 2019).

Here we explore an alternative process which demonstrates how evolution of exposed lithology disrupts drainage networks and creates LRHES. By accounting for contrasts between bedload and bedrock erodibility, we show that even where bedrock strength contrasts are very large, channel steepness values may be relatively uniform across lithological units, thereby obscuring the apparent importance of lithology.

2. Rock Strength Estimates From the Pyrenees

In the case of the Pyrenees, the importance of lithology shaping topography is evidenced by the main drainage divide tracking many of the exposed crystalline basement massifs (Figure 1b; Bernard et al., 2019). Metrics derived to evaluate the erodibility of Pyrenean landscape show a weak correlation with lithology and metric values overlap across different lithologies (Bernard et al., 2019). One metric is based on a model of fluvial elevation through time, dz/dt, responding to rock uplift rate, u, and erosion rate, e. In the stream power model, e is the

product of the upstream drainage area, A and the local channel slope, S, raised to the powers of m and n, respectively (Howard, 1994) and erodibility, K, which encompasses bedrock strength, bedload, hydraulic parameters and climate. Therefore,

$$\frac{dz}{dt} = u - KA^m S^n \tag{1}$$

At close to steady-state, as may be expected for an inactive mountain range in which rock uplift is driven by isostatic compensation to erosion like the Pyrenees, $dz/dt \sim 0$, and $u = KA^m S^n$. This is commonly rearranged in terms of a normalized channel steepness index $k_{sn} = A^{m/n}S$, where m/n = 0.3–0.8 (Mudd et al., 2018), which provides an estimate of the spatial variability in u or K (Kirby & Whipple, 2012). A limitation with this approach is that maps of k_{sn} can be very noisy because calculating slopes from DEMs accentuates noise. Therefore, methods are required to smooth and average the data so that coherent signals can be extracted from the noise. Here we use the approach of Fox (2019) to extract robust values of k_{sn} (Figure 2a) as this approach is less sensitive to noise (Smith et al., 2022). k_{sn} values are similar across the massifs and the surrounding rock (Figure 2b). This is unexpected considering the correlation between k_{sn} and lithology in the similarly post-orogenic southern Appalachian Mountains (Gallen, 2018). We also show that normalized channel steepness values calculated on a pixel-by-pixel basis show no clear correlation with lithology. Furthermore, the uplift rate values are expected to be similar across the Pyrenees and this suggests that the local erodibility, K, is varying.

The relative strength of the two dominant lithologies in the Pyrenees was measured with a Schmidt Hammer by Bernard et al. (2019), which gives an estimate of the compressive strength. The plutonic rocks have a rock compressive strength of about 50 MPa while for the sedimentary rocks the compressive strength is about 25 MPa. The relationship between compressive strength and tensile strength is roughly linear and therefore, despite the inherent limitations of the Schmidt Hammer, we assume that the tensile strength difference between the plutonic rocks and surrounding country rocks varies by a factor of two. Therefore, there is a clear discrepancy between the expected variability in the erodibility if compressive strength is a suitable proxy for erodibility.

The importance of bedload in driving river incision has been described mechanistically and measured in laboratories (Sklar and Dietrich, 2001). These experiments showed that the grainsize and sediment flux control erosion rate and this has been supported by field data (Brocard et al., 2016; Callahan et al., 2019; Finnegan et al., 2017; Johnson et al., 2009; Shobe et al., 2018). However, there is no evidence that grainsize varies with lithology within sedimentary rocks deposited at the time of Pyrenean Orogenesis (Michael et al., 2013).

In summary, the four key observations that motivate our model are: (a) patchy low-relief, high-elevation topography with evidence for transient incision; (b) drainage divides are tortuous and generally coincident with harder plutonic rocks; (c) contrasts in Schmidt Hammer measurements between the two dominant rock types; and (d) k_{sn} variations are comparable between the two dominant lithologies. Our model is based on allowing K to evolve through time as a function of the contrast between the bedrock and bedload erodibility values. This means that the effective erodibility is very variable within a lithological unit, obscuring k_{sn} -lithology variations. In turn, drainages networks are disrupted due to evolving short-wavelength changes in local erosion rates, producing tortuous divides that tend to coincide with the lower erodibility plutons.

3. A Simple Model Accounting for Bedrock-Bedload Contrasts

The expected erosion due to the impact between a particle being transported by a river and the underlying bedrock can be written as a function of the bedrock and particle strength (Sklar and Dietrich, 2004). In particular, the resistance of bedrock to erosion by impacting particles, ε_v, can be written as

$$\varepsilon_v = \frac{k_v \sigma_T^2}{2Y} \tag{2}$$

where σ_T is the tensile strength of the bedrock, Y is the Young's Modulus of elasticity of the bedrock and k_v is a dimensionless coefficient that depends on the material properties of the impacting particle (Engle, 1978). For our illustrative model, in which we are trying to explore the impacts on how changes in outcrop through time may change downstream erodibility, we make the simplifying assumption that the channel erodibility is inversely proportional to this resistance. So, the erodibility is given by

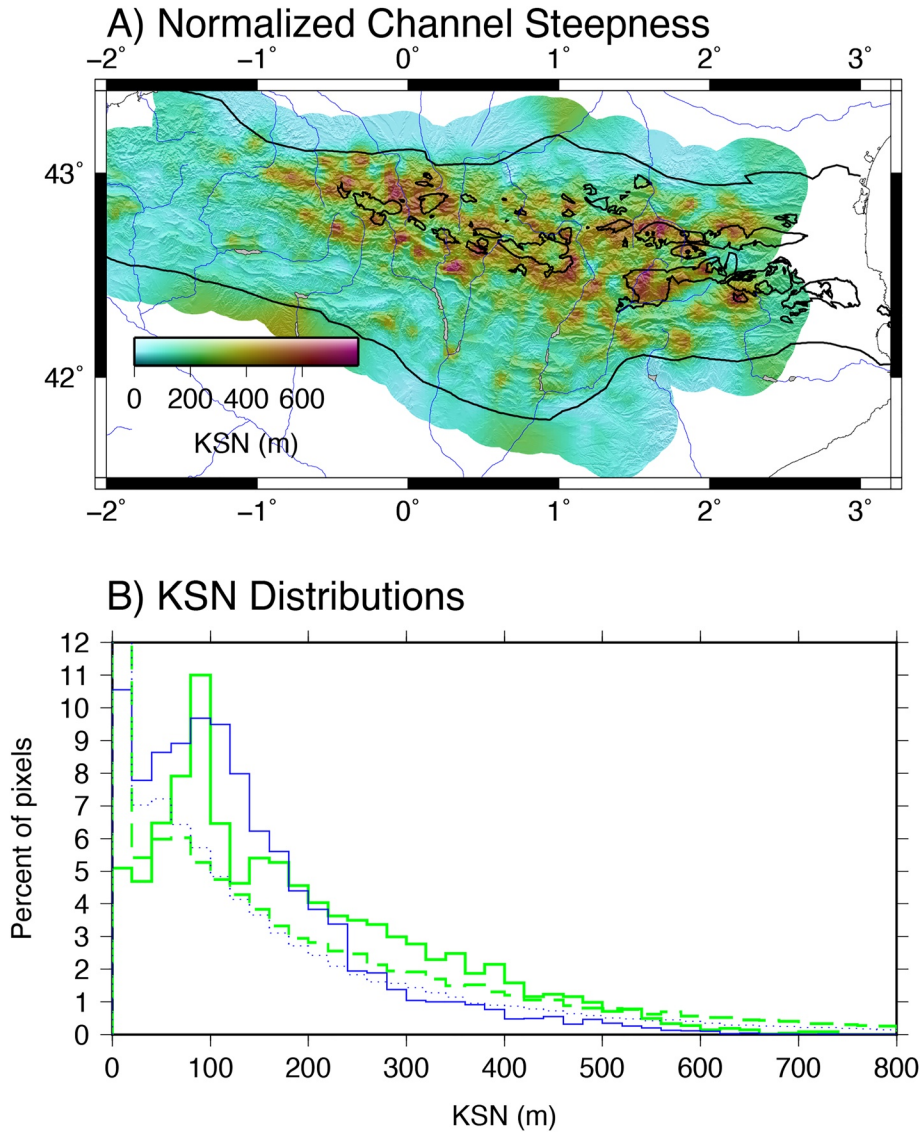

Figure 2. Normalized channel steepness values as a function of lithology. (a) Normalized channel steepness values are calculated using the method of Fox (2019). This method regresses a variable channel steepness map through the relationship between χ and elevation keeping the baselevel for each catchment fixed. This result is produced using a pixel size of 2 km × 2 km. Half of all fluvial nodes with an upstream drainage area greater than 5 km^2 were randomly selected for the simplified topographical data set inversion resulting in a total of 77760 data points. A value of $m = 0.45$ and a smoothing parameter of 5 were used. (b) The distribution of normalized channel steepness values for pixels in the simplified data set. At each node in the simplified data set a channel steepness value from the inversion is extracted. The histograms of the resulting normalized channel steepness values show that across the massifs (green histogram), there is a slight shift toward higher channel steepness values, compared to the surrounding units (blue histogram). If we assume that rock uplift rates are similar across the entire orogen, these differences can be explained by bedrock erodibility contrasts: higher channel steepness values correspond to lower erodibility. The dashed and dotted lines show the same result with no smoothing and show a similar shift toward higher k_{sn} values for the massifs.

$$K = \frac{K_c}{k_v \sigma_T{}^2} \tag{3}$$

where K_c is a constant of proportionality and includes the Young's modulus, which is assumed to be constant.

Based on the Schmidt Hammer by Bernard et al. (2019), the tensile strength difference between the plutonic rocks and surrounding country rocks varies by a factor of two. If erodibility is proportional to $1/\sigma_T{}^2$ (Equation 2), the

erodibility of the plutonic bedrock is approximately four times less than the erodibility of the country rock. We term this contribution to the erodibility K_r and the plutonic erodibility is $K_r(p)$ and the country rock erodibility is $K_r(c)$. In addition, based on the similarity between channel steepness values across the granitic and county rocks, we can say that the erodibility for the plutonic rocks with plutonic bedload is equal to the country rocks with country rock bedload:

$$K = \frac{K_c\, K_r(p)}{k_v(p)} = \frac{K_c K_r(c)}{k_v(c)} \tag{4}$$

which can be rearranged to give,

$$K_r(p)/k_v(p) = K_r(c)\,/k_v(c) \tag{5}$$

The simplest solution to this is that $k_v(p)$ is equal to $K_r(p)$ and that $k_v(c)$ is equal to $K_r(p)$. This suggests that the material properties of the bedload can be taken as the erodibility of the bedrock. More generally we can say that the local erodibility K is equal to

$$K = \frac{K_c * K_r}{K_s} \tag{6}$$

where K_c is simply a scaling parameter. The value of K_s is simply taken from the average erodibility of the bedrock upstream of a specific location, as shown in Figure 3. Similarly, K_r is the erodibility of the local bedrock. In this way, we do not actually track the bedload but assume that it quickly equilibrates to represent the upstream bedrock lithology.

In order to simulate the progressive outcropping of plutonic rocks, oblate spheres of low bedrock erodibility are exhumed toward the surface (Scherler & Schwanghart, 2020), driving river network reorganization (Bernard et al., 2021). The size of our landscape evolution model is similar to the overall size of the Pyrenees. The rock uplift rate is set to 1 km/Ma as a compromise between the pulses of rapid exhumation during the Oligocene and the low exhumation rates since (Fitzgerald et al., 1999; Gibson et al., 2007; Gunnell et al., 2009). The constant erodibility parameter (K_c) is chosen to result in approximately 2 km of relief as observed in the Pyrenees today. The number of plutons is chosen to result in a modern-day distribution similar to what is observed in the Pyrenees, and these are located randomly in time and space. The value of n is set equal to one to highlight the first order influence of accounting for bedload composition in drainage network reorganization during landscape evolution. We acknowledge this is a simplification but it is sufficient to highlight our basic concept. In particular, Perne et al. (2017) show that the value of n is not equal to one, the slope of the contact between lithologies can control local incision using elegant numerical models. However, at the scale of our model, all lithological boundaries are assumed to be vertical. The area exponent, m, is equal to one half, and we include a diffusion term in our landscape evolution model to account for hillslope processes resulting in a mass balance equation:

$$\frac{dz}{dt} = u - \mathrm{K}\mathrm{A}^m \frac{dz}{dl} - \kappa \nabla^2 z \tag{7}$$

where dz/dl is the local slope in the direction of maximum slope and $\nabla^2 z$ is two-dimensional curvature. The erodibility, K, is given by Equation 7 and κ is the diffusivity and is equal to 1×10^{-2} m^2/a. This model is solved across all parts of the landscape evolution model. We discretize space into pixels of size 1 km × 1 km, the model runs for 5 Ma with time steps of 0.01 Ma. We use the Fastscape algorithm to solve for elevations through time (Braun & Willett, 2013).

4. Results

The difference between the erodibility of the plutons (1.25 1/Ma) and country rock (5 1/Ma) is large (Figure 3b), and local variations in K can be even larger (Figure 3c) but a clear correlation between k_{sn} and bedrock lithology is not observed. Evolving differences in the erodibility lead to local changes in erosion rate (Figure 4). For example, when a point on the river network within the country rock has plutonic rock upstream, the bedload is made up of the hard plutonic rock and the bedrock is made up of the softer country rock. This produces an effective erodibility value of up to 20 1/Ma which produces high local erosion rates. These erosion rate variations lead to elevation changes and drainage network reorganization. When the disruption of drainage networks

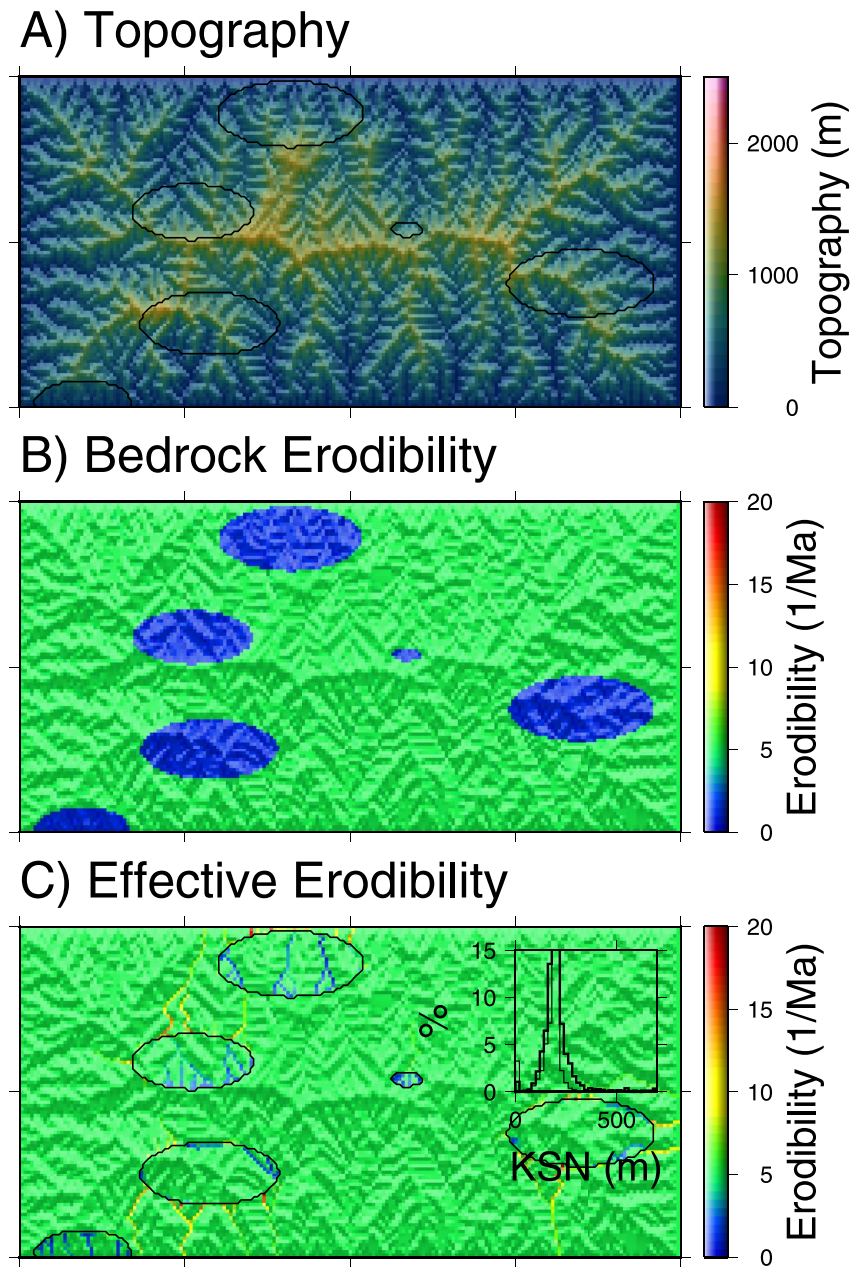

Figure 3. Snapshot of the evolving erodibility values at 5 Myr. (a) The scale of the topography is similar to the Pyrenees. The black lines demark the outlines of the plutons. (b) The bedrock erodibility values of the plutons and the country rock. (c) The erodibility values used in the stream power model is a function of the local contrast between the bedload and the bedrock erodibility. At some locations low erodibility bedload is transported over country rock, resulting in high erodibility values. At other locations the opposite is true. The inset shows that the normalized channel steepness values for the two lithologies are similar and this is to be expected given the similarity in erodibility values.

results in reductions in upstream area, fluvial erosion decreases, yet hillslope processes continue to operate, thereby reducing local relief (Yang et al., 2015). The surfaces, highlighted by the areas of low erosion rate (Figure 4), are found in both the plutonic rocks and the country rock. Once these surfaces have formed, they are then incised into as has been observed in the Pyrenees (Uzel et al., 2019; Figure 1d). In the Pyrenees, the calculated drainage divides tend to follow plutons (Bernard et al., 2019), in our models ~1% of the outcropping country rock compared to ~5% of the plutonic rock has zero upstream drainage area. This shows that the plutonic rocks are more likely to form drainage divides without having a k_{sn} signature of a much harder rock. Importantly, when bedrock differences in erodibility are used as the effective erodibility and bedload-bedrock

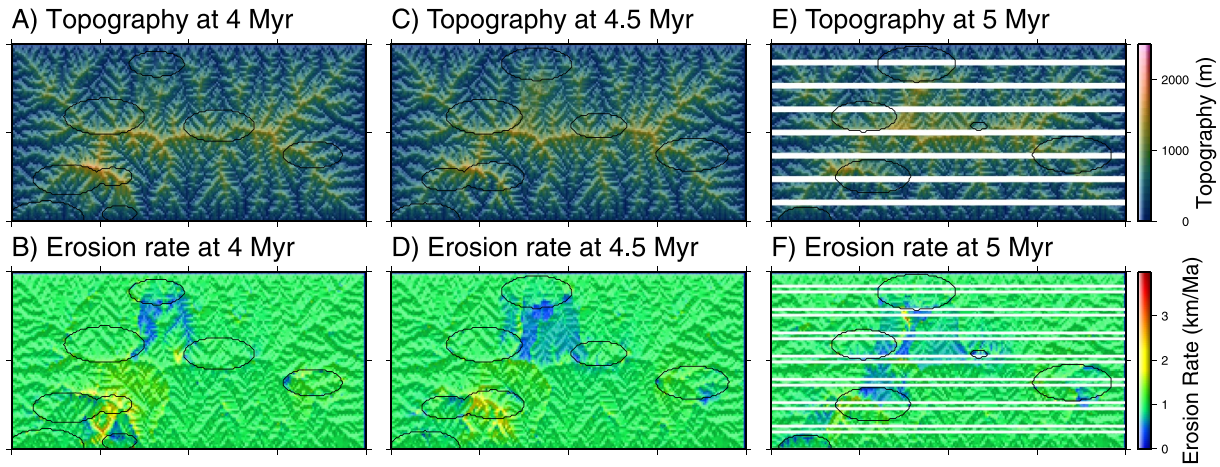

Figure 4. Evolving topography resulting from divide migration. The figure is arranged as 3 timesteps. On the left, topography and erosion rates are shown for 4 Myr of model runtime. The central pair of figures shows the topography and erosion rates at 4.5 Myr and the right pair, at 5 Myr. In all panels, there are areas of low erosion rate, both large areas forming low-relief surfaces and small areas that are preserved from previous time steps. From 4.5 to 5 Myr, the small pluton in the north is exhumed and blocks off a large area. Here, fluvial erosion rates drop while hillslope diffusion continues. In addition, at 5 Myr two plutons in the south east have joined and the smaller of the two plutons is dragging the divide to the south, as shown by asymmetric erosion rates across the divide immediately to the north.

contrasts are not accounted for, k_{sn} values strongly depend on lithology. Furthermore, spatial variations in erodibility are reduced from varying between >1 and ~20 1/Ma in Figure 3c to 1.25 to 5 1/Ma in Figure 5c. This reduction in the variability of erodibility reduces the spatial variability in erosion rates. Ultimately, spatial variability in erosion rates across drainage divides disrupts the drainage network and thus when erodibility only varies as a function of bedrock lithology, drainage divides are not so dynamic (Figures 5 and 6). This reduction in divide dynamism, shown by reduced low-erosion rate locations, reduces the chance of LRHES formation.

5. Discussion and Conclusions

Our simple model reproduces several of the key features of the topography of the high Pyrenees and does not require complex changes in boundary conditions (Figures 3 and 4). Instead, we rely on superficial changes in outcropping lithology and on steady tectonic forcing. This relatively steady tectonic forcing is supported by post-orogenic flexural modeling (Curry et al., 2019). Overall, drainage divides are most likely to be found within the low erodibility plutons in our model, as is the case with the massifs of the Pyrenees. Furthermore, bedload contrasts obscure trends between lithology and normalized channel steepness, despite large differences in relative strength between lithologies. The degree to which the locations of the plutons control the positions of the drainage divides depends on the time that the plutons appear at the surface and the erodibility contrasts imposed in the model. The size of the plutons, the background rock uplift rate and the erodibility contrast between the plutons and the country rocks will all influence these outcomes, but the simple conclusions of our analysis are robust across a suite of model configurations tested.

This new mechanism for the formation of LRHES is driven by lithological contrasts between bedload and bedrock erodibilities and the resulting drainage network reorganization. Traditional mechanisms to create these surfaces have required large scale geodynamic events such as peneplanation close to sea level followed by rock uplift (Gunnell et al., 2008) or km-scale changes in fluvial baselevel (Babault et al., 2005). In other locations, recent research has deviated from these concepts and suggests continued tectonic evolution can drive drainage network reorganization to produce LRHES but these have still been based on spatial changes in rock uplift (Yuan et al., 2022) or changes in tectonic shortening (Yang et al., 2015). In contrast, our mechanism is based on steady tectonic processes with evolving lithology, creating drainage divides pinned to plutonic rocks but no clear lithological signature in k_{sn} values. More generally, our two-dimensional landscape evolution model highlights how bedload composition evolution sets incision rates and, ultimately, drives drainage network reorganization. It is therefore important that resulting k_{sn} variations from processes related to changing upstream areas are not mistaken for signatures of lithology or tectonic control on river incision.

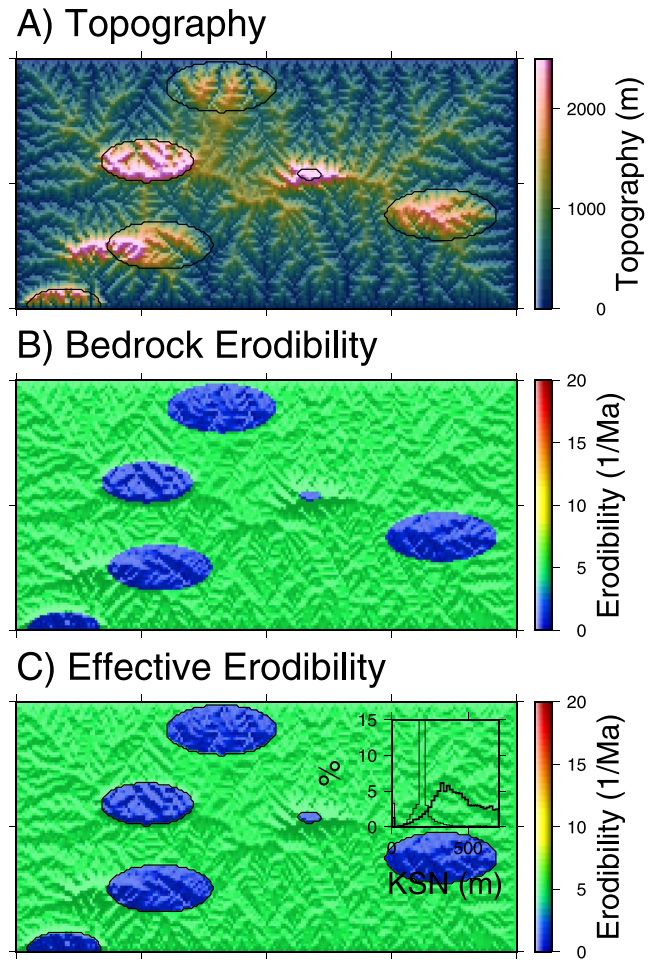

Figure 5. If the effective erodibility is simply a function of the bedrock lithology, the lithology has a clear impact on the channel steepness. This is shown in the insert in (c). The layout of the figure is the same as Figure 3. The effective erodibility is less variable compared to Figure 3c and varies between 1.25 and 5 1/Ma. This change in erodibility leads to systematic patterns in erosion rate between the two lithologies producing distinct channel steepness signatures. The variability in the channel steepness values observed in the insert is the result of the evolution of outcropping lithology and drainage network reorganization.

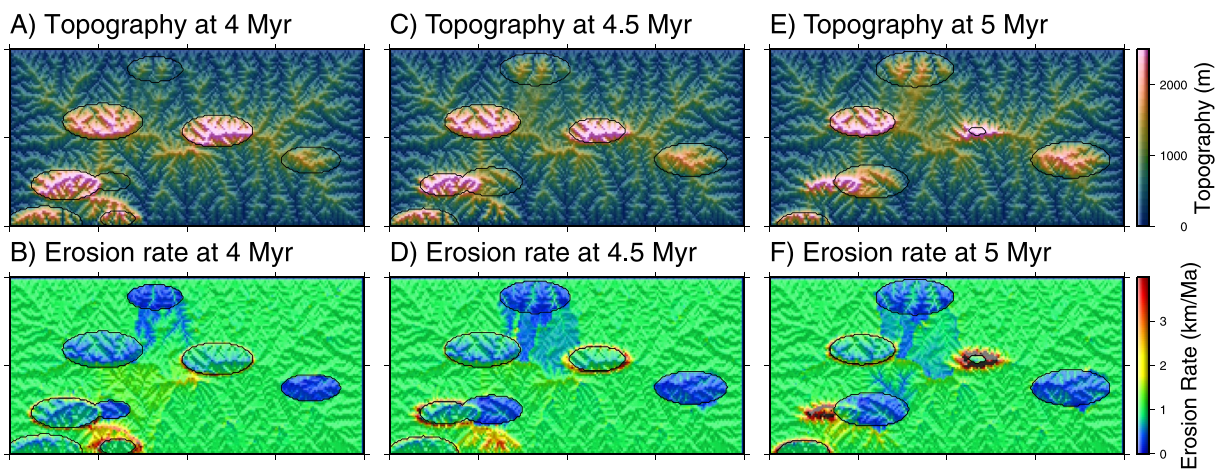

Figure 6. If the effective erodibility is simply a function of the bedrock lithology the overall topography is clearly a function of the lithology, with plutonic units forming the highest parts of the landscape. In this way, the drainage network is also very dependent on the lithology. In addition, the drainage network is less dynamic and the mechanism of lithological variations forming high elevation surfaces that cut through different lithological units is less effective due to the reduction in the range of effective erodibility. The layout is the same as Figure 4.

Data Availability Statement

No new data were generated for this study. Schmidt Hammer data are available from https://doi.org/10.1016/j.epsl.2019.04.034 and DEM data are from Hydrosheds (https://doi.org/10.1029/2008eo100001).

Acknowledgments
We thank A. Carter and J. Turowski for stimulating discussion. This study was greatly improved thanks to review comments from S. Gallen, J. Gosse and an anonymous reviewer. MF was supported by NERC (NE/N015479/1).

References

Babault, J., Van Den Driessche, J., Bonnet, S., Castelltort, S., & Crave, A. (2005). Origin of the highly elevated Pyrenean peneplain. *Tectonics*, *24*(2), TC2010. https://doi.org/10.1029/2004TC001697

Bernard, T., Sinclair, H. D., Gailleton, B., Mudd, S. M., & Ford, M. (2019). Lithological control on the post-orogenic topography and erosion history of the Pyrenees. *Earth and Planetary Science Letters*, *518*, 53–66. https://doi.org/10.1016/j.epsl.2019.04.034

Bernard, T., Sinclair, H. D., Naylor, M., Christophoul, F., & Ford, M. (2021). Post-orogenic sediment drape in the Northern Pyrenees explained using a box model. *Basin Research*, *33*(1), 118–137. https://doi.org/10.1111/bre.12457

Bosch, G. V., Van den Driessche, J., Babault, J., Robert, A., Carballo, A., Le Carlier, C., et al. (2016). Peneplanation and lithosphere dynamics in the Pyrenees. *Comptes Rendus Geoscience*, *348*(3–4), 194–202. https://doi.org/10.1016/j.crte.2015.08.005

Braun, J., & Willett, S. D. (2013). A very efficient O(*n*), implicit and parallel method to solve the stream power equation governing fluvial incision and landscape evolution. *Geomorphology*, *180*, 170–179. https://doi.org/10.1016/j.geomorph.2012.10.008

Brocard, G. Y., Willenbring, J. K., Miller, T. E., & Scatena, F. N. (2016). Relict landscape resistance to dissection by upstream migrating knickpoints. *Journal of Geophysical Research: Earth Surface*, *121*(6), 1182–1203. https://doi.org/10.1002/2015JF003678

Cabrera, L., Roca, E., & Santanach, P. (1988). Basin formation at the end of a strike-slip fault: The Cerdanya basin (eastern Pyrenees). *Journal of the Geological Society*, *145*(2), 261–268. https://doi.org/10.1144/gsjgs.145.2.0261

Callahan, R. P., Ferrier, K. L., Dixon, J., Dosseto, A., Hahm, W. J., Jessup, B. S., et al. (2019). Arrested development: Erosional equilibrium in the southern Sierra Nevada, California, maintained by feedbacks between channel incision and hillslope sediment production. *Bulletin*, *131*(7–8), 1179–1202. https://doi.org/10.1130/B35006.1

Calvet, M. (1996). *Morphogenèse d'une montagne méditerranéenne: les Pyrénées orientales* (Thèse d'État, document du BRGM) (Vol. *255*).

Curry, M. E., van der Beek, P., Huismans, R. S., Wolf, S. G., & Muñoz, J. A. (2019). Evolving paleotopography and lithospheric flexure of the Pyrenean Orogen from 3D flexural modeling and basin analysis. *Earth and Planetary Science Letters*, *515*(1), 26–37. https://doi.org/10.1016/j.epsl.2019.03.009

Davis, W. M. (1899). The geographical cycle. *The Geographical Journal*, *14*(5), 481. https://doi.org/10.2307/1774538

de Sitter, L. U. (1952). Pliocene uplift of Tertiary mountain chains. *American Journal of Science*, *250*(4), 297–307. https://doi.org/10.2475/ajs.250.4.297

England, P., & Molnar, P. (1990). Surface uplift, uplift of rocks, and exhumation of rocks. *Geology*, *18*(12), 1173–1177. https://doi.org/10.1130/0091-7613(1990)018<1173:SUUORA>2.3.CO;2

Engle, P. A. (1978). *Impact wear of materials*. Elsevier Science.

Finnegan, N. J., Klier, R. A., Johnstone, S., Pfeiffer, A. M., & Johnson, K. (2017). Field evidence for the control of grain size and sediment supply on steady-state bedrock river channel slopes in a tectonically active setting. *Earth Surface Processes and Landforms*, *42*(14), 2338–2349. https://doi.org/10.1002/esp.4187

Fitzgerald, P. G., Muñoz, J. A., Coney, P. J., & Baldwin, S. L. (1999). Asymmetric exhumation across the Pyrenean orogen: Implications for the tectonic evolution of a collisional orogen. *Earth and Planetary Science Letters*, *173*(3), 157–170. https://doi.org/10.1016/S0012-821X(99)00225-3

Fox, M. (2019). A linear inverse method to reconstruct paleo-topography. *Geomorphology*, *337*, 151–164. https://doi.org/10.1016/j.geomorph.2019.03.034

Gallen, S. F. (2018). Lithologic controls on landscape dynamics and aquatic species evolution in post-orogenic mountains. *Earth and Planetary Science Letters*, *493*, 150–160. https://doi.org/10.1016/j.epsl.2018.04.029

Gibson, M., Sinclair, H. D., Lynn, G. J., & Stuart, F. M. (2007). Late-to post-orogenic exhumation of the Central Pyrenees revealed through combined thermochronological data and modelling. *Basin Research*, *19*(3), 323–334. https://doi.org/10.1111/j.1365-2117.2007.00333.x

Gunnell, Y., & Calvet, M. (2006). Comment on "Origin of the highly elevated Pyrenean peneplain" by Julien Babault, Jean Van Den Driessche, and Stéphane Bonnet, Sébastien Castelltort, and Alain Crave. *Tectonics*, *25*(3). https://doi.org/10.1029/2004TC001697

Gunnell, Y., Calvet, M., Brichau, S., Carter, A., Aguilar, J. P., & Zeyen, H. (2009). Low long-term erosion rates in high-energy mountain belts: Insights from thermo-and biochronology in the Eastern Pyrenees. *Earth and Planetary Science Letters*, *278*(3–4), 208–218. https://doi.org/10.1016/j.epsl.2008.12.004

Gunnell, Y., Zeyen, H., & Calvet, M. (2008). Geophysical evidence of a missing lithospheric root beneath the Eastern Pyrenees: Consequences for post-orogenic uplift and associated geomorphic signatures. *Earth and Planetary Science Letters*, *276*(3–4), 302–313. https://doi.org/10.1016/j.epsl.2008.09.031

Howard, A. D. (1994). A detachment-limited model of drainage basin evolution. *Water Resources Research*, *30*(7), 2261–2285. https://doi.org/10.1029/94wr00757

Johnson, J. P., Whipple, K. X., Sklar, L. S., & Hanks, T. C. (2009). Transport slopes, sediment cover, and bedrock channel incision in the Henry Mountains, Utah. *Journal of Geophysical Research*, *114*(F2), F02014. https://doi.org/10.1029/2007JF000862

Kirby, E., & Whipple, K. X. (2012). Expression of active tectonics in erosional landscapes. *Journal of Structural Geology*, *44*, 54–75. https://doi.org/10.1016/j.jsg.2012.07.00

Lehner, B., Verdin, K., & Jarvis, A. (2008). New global hydrography derived from spaceborne elevation data. *Eos, Transactions, American Geophysical Union*, *89*(10), 93–94. https://doi.org/10.1029/2008eo100001

Michael, N. A., Whittaker, A. C., & Allen, P. A. (2013). The functioning of sediment routing systems using a mass balance approach: Example from the Eocene of the southern Pyrenees. *The Journal of Geology*, *121*(6), 581–606. https://doi.org/10.1086/673176

Mudd, S. M., Clubb, F. J., Gailleton, B., & Hurst, M. D. (2018). How concave are river channels? *Earth Surface Dynamics*, *6*(2), 505–523. https://doi.org/10.5194/esurf-6-505-2018

Ortuño, M., Martí, A., Martín-Closas, C., Jiménez-Moreno, G., Martinetto, E., & Santanach, P. (2013). Palaeoenvironments of the late Miocene Prüedo basin: Implications for the uplift of the central Pyrenees. *Journal of the Geological Society*, *170*(1), 79–92. https://doi.org/10.1144/jgs2011-121

Ortuño, M., Queralt, P., Martí, A., Ledo, J., Masana, E., Perea, H., & Santanach, P. (2008). The North Maladeta Fault (Spanish Central Pyrenees) as the Vielha 1923 earthquake seismic source: Recent activity revealed by geomorphological and geophysical research. *Tectonophysics*, *453* (1-4), 246–262. https://doi.org/10.1016/j.tecto.2007.06.016

Perne, M., Covington, M. D., Thaler, E. A., & Myre, J. M. (2017). Steady state, erosional continuity, and the topography of landscapes developed in layered rocks. *Earth Surface Dynamics*, *5*(1), 85–100. https://doi.org/10.5194/esurf-5-85-2017

Roca, E. (1996). E10 the Neogene Cerdanya and Seu d'Urgell intramontane basins (eastern Pyrenees). In *Tertiary basins of Spain: The stratigraphic record of crustal kinematics* (pp. 114–119). Cambridge University Press.

Scherler, D., & Schwanghart, W. (2020). Drainage divide networks–Part 2: Response to perturbations. *Earth Surface Dynamics*, *8*(2), 261–274. https://doi.org/10.5194/esurf-8-261-2020

Shobe, C. M., Tucker, G. E., & Rossi, M. W. (2018). Variable-threshold behavior in rivers arising from hillslope-derived blocks. *Journal of Geophysical Research: Earth Surface*, *123*(8), 1931–1957. https://doi.org/10.1029/2017JF004575

Sklar, L. S., & Dietrich, W. E. (2001). Sediment and rock strength controls on river incision into bedrock. *Geology*, *29*(12), 1087–1090. https://doi.org/10.1130/0091-7613(2001)029<1087:SARSCO>2.0.CO;2

Sklar, L. S., & Dietrich, W. E. (2004). A mechanistic model for river incision into bedrock by saltating bed load. *Water Resources Research*, *40*(6), W06301. https://doi.org/10.1029/2003WR002496

Smith, A. G., Fox, M., Schwanghart, W., & Carter, A. (2022). Comparing methods for calculating channel steepness index. *Earth-Science Reviews*, *227*, 103970. https://doi.org/10.1016/j.earscirev.2022.103970

Uzel, J., Nivière, B., & Lagabrielle, Y. (2019). Fluvial incisions in the north-western Pyrenees (Aspe valley, France): Dissection of a former Planation surface and some tectonic implications. *AGU Fall Meeting Abstracts*, *2019*, EP31C–2300. https://doi.org/10.1111/ter.12431

Yang, R., Willett, S. D., & Goren, L. (2015). In situ low-relief landscape formation as a result of river network disruption. *Nature*, *520*(7548), 526–529. https://doi.org/10.1038/nature14354

Yuan, X. P., Huppert, K. L., Braun, J., Shen, X., Liu-Zeng, J., Guerit, L., et al. (2022). Propagating uplift controls on high-elevation, low-relief landscape formation in the southeast Tibetan Plateau. *Geology*, *50*(1), 60–65. https://doi.org/10.1130/G49022.1